PHYSICAL REVIEW E **71**, 056620 (2005)

Bistability in the sine-Gordon equation: The ideal switch

R. Khomeriki[1,2] and J. Leon[1]
[1]*Laboratoire de Physique Théorique et Astroparticules CNRS-UMR5207, Université Montpellier 2, 34095 Montpellier, France*
[2]*Physics Department, Tbilisi State University, 0128 Tbilisi, Georgia*
(Received 25 January 2005; published 27 May 2005)

The sine-Gordon equation, used as the representative nonlinear wave equation, presents a bistable behavior resulting from nonlinearity and generating hysteresis properties. We show that the process can be understood in a comprehensive analytical formulation and that it is a generic property of nonlinear systems possessing a natural band gap. The approach allows one to discover that the sine-Gordon equation can work as an *ideal switch* by reaching a transmissive regime with vanishing driving amplitude.

DOI: 10.1103/PhysRevE.71.056620 PACS number(s): 05.45.Yv, 03.75.Lm

I. INTRODUCTION

A nonlinear medium submitted to wave irradiation at a frequency in a forbidden band gap can undergo bistable behavior and present hysteresis properties. This bistability has attracted much attention, e.g., in nonlinear optics as a means for a medium to switch from total reflection to partial (sometimes total) transmission [1] or in superconducting junction devices as a means to conceive amplifiers that "remain efficient in the quantum limit" [2]. We attempt to give a comprehensive interpretation of this phenomenon in terms of both analytical description and numerical simulations, in order to unveil a particular stationary regime presenting a nonzero output for vanishing input, which we call the ideal switch and which allows for detection of (almost) vanishing signal.

To that end we consider the sine-Gordon equation on the finite interval $x \in [0,L]$

$$u_{tt} - u_{xx} + \sin u = 0, \tag{1}$$

associated to the boundary value problem

$$u(0,t) = f(t), \quad u_x(L,t) = 0, \tag{2}$$

on a vanishing initial state [with $f(0)=0$ and $f_t(0)=0$ for compatibility of the initial and boundary values].

This is a quite standard problem in physics of a wave equation with a forced extremity (Dirichlet boundary condition in $x=0$) and a free end (Neumann boundary condition in $x=L$), associated to Cauchy initial data at $t=0$. A related physical situation is, for instance, a long Josephson junction [3,4] or an array of coupled short junctions (Josephson superlattice) [5,6]. Note that, depending on the used external driving, the boundary (2) possibly has to be replaced with $u_x(0,t)$.

An important subclass of boundary $f(t)$ is constant amplitude periodic driving at a frequency in the natural band gap of the system, namely,

$$f(t) = B_0 \cos(\Omega t), \quad \Omega < 1, \tag{3}$$

after a convenient transient sequence where $f(t)$ grows from a vanishing amplitude to the value B_0 to avoid initial shock. While for a linear system this boundary excitation does not flow through, nonlinearity allows for energy transmission above the threshold amplitude which reads (in the semi-infinite case $L \to \infty$)

$$B_s = 4\arctan(b_s), \quad b_s^2 = \frac{1-\Omega^2}{\Omega^2}. \tag{4}$$

This is called nonlinear supratransmission [7] and happens by emission of solitons (moving breathers) that propagate in the nonlinear medium.

This process, quite generic, has been experimentally realized on a chain of coupled pendula [8], and applies, for instance, in discrete systems of coupled waveguide arrays [9] where the forbidden gap results from discreteness, or else in Bragg media (periodic dielectric structures) under constant microwave irradiation in the photonic band gap [10]. In Josephson junctions arrays, submitted to microwave excitation, the boundary $u_x(0,t)=f(t)$ induces the threshold $B_s=2(1-\Omega^2)$ [8].

In the finite line case considered here, we shall again find a nonlinear supratransmission threshold which tends to the value (4) for large L. But a property far less understood is the hysteresis loop obtained by decreasing the amplitude excitation B_0 from the threshold B_s. This property has been for instance observed on numerical simulations [5,6] in the context of Josephson superlattices, but both the analytical expression of the threshold and the very nonlinear mechanism involved have not been clarified.

We shall establish a general procedure to determine the threshold by studying the standing periodic solutions of the sine-Gordon equation which synchronize to the driving frequency Ω and adapts to the driving amplitude B_0. Although these two conditions are sufficient to determine the solution completely, it is not uniquely defined. Indeed we shall prove that a fixed set of physical parameters $\{L,\Omega,B_0\}$ may be related to more than one solution. This is the principle that leads to bistability when $B_0 < B_s$.

As an interesting consequence we obtain that there exists a regime where a vanishing input amplitude B_0 produces a nonvanishing output amplitude. This process shows that the sine-Gordon equation can be thought of as an ideal switch along the hysteresis loop from zero to zero input amplitudes.

The paper is organized as follows. In the next section we display the set of explicit solutions to the sine-Gordon equation on a length L submitted to the only requirements that the input boundary amplitude be B_0 and the period of the solution be $2\pi/\Omega$. The following section is devoted to the analytical definition and evaluation of the threshold of bistability. Then we show by numerical simulations in Sec. IV that those explicit solution are indeed produced by the boundary driving (3) and we check bistability predictions. In particular we compute, for a more realistic damped sine-Gordon model, the power released by the boundary driver to the medium and find that after having switched, this power is 2 to 3 orders of magnitude larger than before the switch.

II. EXPLICIT SOLUTIONS

A. General expressions

Under boundary condition (3), in order to describe the periodic asymptotic regime reached in numerical simulations, we follow Ref. [11] and seek a solution

$$u(x,t) = 4\arctan[X(x)T(t)]. \tag{5}$$

The boundary condition in $u_x(L,t)=0$ then reads

$$X'(L) = 0, \quad X(L) = A, \tag{6}$$

where we have defined the amplitude parameter A such as to scale $T(t)$ to unity. In other words

$$\exists t_0\colon T'(t_0) = 0, \quad T(t_0) = 1. \tag{7}$$

By inserting expression (5) in the sine-Gordon equation (1) and by use of constraints (6) and (7), we obtain differential equations with a unique free parameter α:

$$(X')^2 = \alpha\Gamma(A^2 - X^2)\left(X^2 + \frac{1}{\Gamma A^2}\right), \tag{8}$$

$$(T')^2 = \alpha(1 - T^2)(T^2 + \Gamma), \tag{9}$$

where a prime denotes differentiation and where

$$\Gamma = \frac{1}{A^2} + \frac{1}{\alpha(1 + A^2)}. \tag{10}$$

Thanks to Eqs. (6) and (7) the equation for $X(x)$ is integrated on $[x,L]$ and the one for $T(t)$ on $[t,t_0]$. The solution is then completely defined (in terms of elliptic integrals) by the values of the two parameters A and α, determined as follows.

Our first fundamental hypothesis is to assume, accordingly with numerical simulations, that the solution *synchronizes* to the boundary driving, namely, that the function $T(t)$ is periodic with the period of the driver

$$T\left(t + \frac{2\pi}{\Omega}\right) = T(t). \tag{11}$$

The second fundamental hypothesis consists in expressing that the solution *adapts* to the driving amplitude $B_0 = 4\arctan(a)$, which gives

$$X(0) = a. \tag{12}$$

The two relations (11) and (12) constitute a closed system of equations for the two unknowns A and α in terms of the physical constants a, Ω, and L.

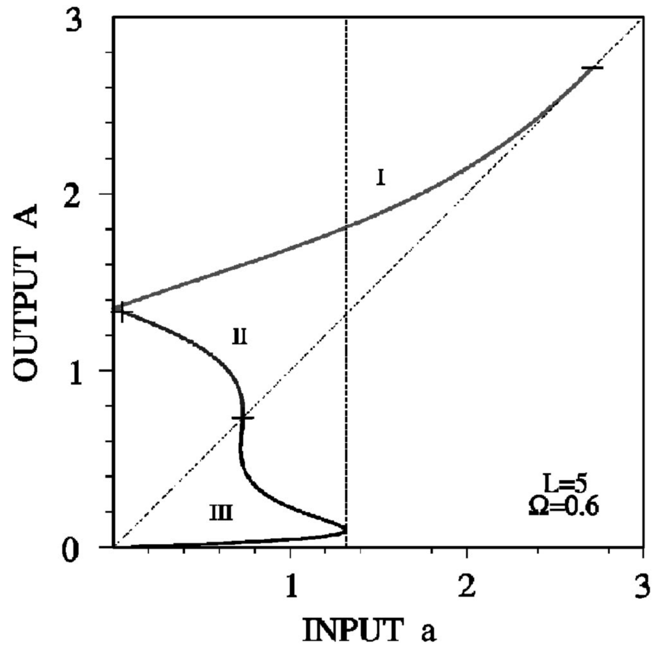

FIG. 1. Plot of the curves $|A(a)|$ in the three cases for $L=5$ and $\Omega=0.6$. The crosses indicate the points where the solution changes from one type to the other. The vertical line shows the threshold amplitude a_s (next section) above which supratransmission occurs by emission of solitons.

The point is that bistability occurs because the solution of Eqs. (8), (9) drastically depends on the sign of α. We shall indeed discover that there may exist different solutions that do synchronize to Ω and adapts to a. In other words, for any fixed Ω and L, a given input amplitude a may correspond to more than one value of the output amplitude A as depicted in Fig. 1.

B. Type I solutions

We call type I solutions those obtained for $\alpha > 0$ (implying $\Gamma > 0$) for which we obtain [12]

$$T(t) = \mathrm{cn}(\omega(t - t_0), \nu), \tag{13}$$

$$X(x) = A\ \mathrm{cn}(k(x - L), \mu), \tag{14}$$

$$\omega^2 = \alpha(1 + \Gamma), \quad \nu^2 = \frac{1}{1 + \Gamma},$$

$$k^2 = \alpha\Gamma\left(A^2 + \frac{1}{\Gamma A^2}\right), \quad \mu^2 = \frac{\Gamma A^4}{1 + \Gamma A^4}. \tag{15}$$

where $\mathrm{cn}(\ldots, m)$ is the cosine-amplitude Jacobi elliptic function of modulus m. According to Ref. [11], the resulting solution $u(x,t)$ is called plasma oscillation and we have from Eq. (15)

$$\omega^2 = k^2 + \frac{1 - A^2}{1 + A^2}. \tag{16}$$

This relation between the nonlinear wave parameters ω and k is often called a nonlinear dišpersion relation but we shall reserve such a denomination to the true dispersion relation which relates the actual period $4\mathbb{K}(\mu)/k$ of $X(x)$ to the period $4\mathbb{K}(\nu)/\omega$ of $T(t)$.

The parameters α and A are now determined by requiring synchronization (11) and input datum (12), namely, here by solving for unknowns α and A the system

$$\Omega\mathbb{K}(\nu) = \frac{\pi}{2}\omega, \quad a = A\ \mathrm{cn}(kL,\mu). \tag{17}$$

[Note that the complete elliptic integral $\mathbb{K}(\nu)$ is well defined as for $\Gamma > 0$ we have $0 < \nu^2 < 1$.]

It is useful to express the above solution in terms of the two wave parameters ω and k. This is done by using Eq. (16) to eliminate A and α from the definitions of μ and ν. We get

$$A^2 = \frac{1-\omega^2+k^2}{1+\omega^2-k^2},$$

$$\nu^2 = \frac{k^4-(\omega^2-1)^2}{4\omega^2},$$

$$\mu^2 = \frac{4k^2}{(1+k^2)^2-\omega^4}. \tag{18}$$

System (17) appears then as an equation for the determination of the parameters ω and k from the data of the length L, the boundary driver's frequency Ω, and amplitude a.

C. Type II solutions

New types of solutions are obtained for $\alpha < 0$ for which the evolution (9) of $T(t)$ requires $\Gamma < 0$ in order to guarantee the constraint (7). Defining

$$\beta = -\alpha, \quad \Lambda = -\Gamma = \frac{1}{\beta(1+A^2)} - \frac{1}{A^2}, \tag{19}$$

the basic equations (8) and (9) become

$$(T')^2 = \beta(1-T^2)(\Lambda - T^2), \tag{20}$$

$$(X')^2 = \beta\Lambda(A^2-X^2)\left(X^2 - \frac{1}{\Lambda A^2}\right). \tag{21}$$

It appears that the constraint (7) which states that $T(t_0)=1$, requires $\Lambda > 1$, namely,

$$\beta < \frac{A^2}{(1+A^2)^2}, \tag{22}$$

a condition that must be checked *a posteriori* when computing β from the synchronization constraint.

The structure of Eq. (1) implies two classes of solutions depending on the relative values of A^2 and $1/(\Lambda A^2)$. Type II solutions are obtained for $\Lambda A^4 > 1$ which, together with constraint (22), reads

$$A^2 > 1{:}\ 0 < \beta < A^2/(1+A^2)^2, \tag{23}$$

$$A^2 < 1{:}\ 0 < \beta < A^4/(1+A^2)^2. \tag{24}$$

The solution of Eqs. (20), (21) can now be obtained as

$$T(t) = \mathrm{sn}(\omega(t-t_1),\nu), \quad t_1 = t_0 + \mathbb{K}(\nu)/\omega, \tag{25}$$

$$X(x) = A\ \mathrm{dn}(k(x-L),\mu), \tag{26}$$

$$\omega^2 = \beta\Lambda, \quad \nu^2 = \frac{1}{\Lambda},$$

$$k^2 = \beta\Lambda A^2, \quad \mu^2 = 1 - \frac{1}{\Lambda A^4}, \tag{27}$$

and we have the relation

$$\omega^2 = \frac{k^2}{A^2} \tag{28}$$

between the wave parameters k and ω for the type II solution.

The parameters β and A are determined as before by requiring synchronization (11) and input datum (12), namely,

$$\Omega\mathbb{K}(\nu) = \frac{\pi}{2}\omega, \quad a = A\ \mathrm{dn}(kL,\mu). \tag{29}$$

Although the above equation, for real valued parameters, has two sets of solutions $\{\beta, A\}$, only one set verifies the constraint $\Lambda A^4 > 1$.

As before, we express the type II solution in terms of the wave parameters ω and k, by means of Eq. (28) to eliminate A and β in μ and ν. We obtain

$$A^2 = \frac{k^2}{\omega^2},$$

$$\nu^2 = \frac{k^2}{\omega^2}\frac{1-\omega^2-k^2}{\omega^2+k^2},$$

$$\mu^2 = 1 - \frac{\omega^2}{k^2}\frac{1-\omega^2-k^2}{\omega^2+k^2}. \tag{30}$$

System (29) determines then the parameters ω and k from the data of L, Ω, and a.

D. Type III solutions

The type III solution is obtained still for $\alpha < 0$ when $\Lambda A^4 < 1$. Such can be realized only in the case $A^2 < 1$ by requiring

$$A^4/(1+A^2)^2 < \beta < A^2/(1+A^2)^2. \tag{31}$$

The solution of Eqs. (20), (21) now reads

$$T(t) = \mathrm{sn}(\omega(t-t_1),\nu), \quad t_1 = t_0 + \mathbb{K}(\nu)/\omega \tag{32}$$

$$X(x) = A\ \mathrm{dn}^{-1}(k(x-L),\mu), \tag{33}$$

$$\omega^2 = \beta\Lambda, \quad \nu^2 = \frac{1}{\Lambda}, \quad k^2 = \frac{\beta}{A^2}, \quad \mu^2 = 1 - \Lambda A^4, \tag{34}$$

and the wave parameters obey

$$\omega^2 = \frac{1}{1+A^2} - k^2. \tag{35}$$

The synchronization condition (11) and input datum (12) furnish the system

$$\Omega\,\mathbb{K}(\nu) = \frac{\pi}{2}\omega, \quad a = \frac{A}{\mathrm{dn}(kL,\mu)} \tag{36}$$

for the unknowns parameters β and A. The same remark as for the type II solution holds here, namely, that the system (36) has two sets of solutions $\{\beta, A\}$ but only one verifies the constraint $\Lambda A^4 < 1$.

Again the type III solution can be expressed entirely in terms of the two parameters ω and k by means of Eq. (35) which gives

$$A^2 = \frac{1-\omega^2-k^2}{\omega^2+k^2},$$

$$\nu^2 = \frac{k^2}{\omega^2}\frac{1-\omega^2-k^2}{\omega^2+k^2},$$

$$\mu^2 = 1 - \frac{\omega^2}{k^2}\frac{1-\omega^2-k^2}{\omega^2+k^2}. \tag{37}$$

Then Eq. (36) is a system for the parameters ω and k in terms of the data L, Ω, and a.

III. BISTABILITY THRESHOLDS

The above three solutions are now used to describe analytically bistability properties of the sine-Gordon equation. The first step is to define and calculate, at given length L, the threshold a_s as functions of the driving frequency Ω. Last, decreasing the input amplitude from a_s, once a transmission regime has been reached, the system locks to the type-I solution which holds down to a vanishing driving amplitude. This is a property that makes the sine-Gordon equation an ideal switch and allows one to understand how it can be used to detect weak (vanishing) signals.

A. Transmission threshold

As shown in Fig. 1, increasing the input amplitude from $a=0$ generates the type III solution. This solution has, for sufficient length, an approximate maximum input value a_s resulting from Eq. (36) as the point where $\mathrm{dn}(kL,\mu)$ reaches its minimum value $\sqrt{1-\mu^2}$, namely,

$$a_s^2 = \frac{A^2}{1-\mu^2}. \tag{38}$$

Such a definition of the threshold a_s is more conveniently written in terms of ω and k through Eq. (37) as

$$a_s^2 = \frac{k^2}{\omega^2}. \tag{39}$$

In this equation, the parameters ω and k are determined through Eq. (36) which, at the threshold, can also be written as the system

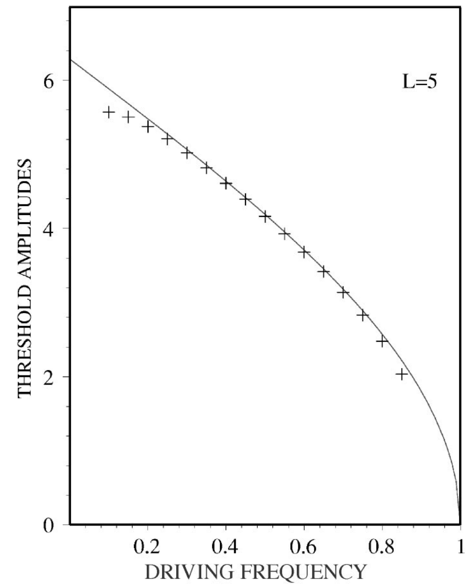

FIG. 2. Input amplitude 4 arctan(a_s) at the threshold, solution of Eqs. (39), (40) as a function of Ω for $L=5$ (crosses) and compared to its limit value 4 arctan(b_s) as $L\to\infty$, given by Eq. (43) (full line).

$$\Omega\,\mathbb{K}(\nu) = \frac{\pi}{2}\omega, \quad kL = \mathbb{K}(\mu), \tag{40}$$

with ν and μ given by Eq. (37).

Figure 2 shows that the threshold a_s is quite close to the expression of b_s in Eq. (4). This property is demonstrated in general by studying the limit $L\to\infty$ in the type III solution. At threshold amplitude, the relation (40) between L and μ gives the necessary condition

$$L\to\infty \Rightarrow \mu\to 1 \Rightarrow \omega^2 \to 1-k^2, \tag{41}$$

with which the synchronization condition provides

$$L\to\infty \Rightarrow \nu\to 0 \Rightarrow \omega\to\Omega. \tag{42}$$

With this in hands, the expression (39) of the threshold readily gives the expression (4), namely,

$$L\to\infty \Rightarrow a_s^2 \to b_s^2 = \frac{1-\Omega^2}{\Omega^2}. \tag{43}$$

Remark. it is instructive to compute also the limit $L\to\infty$ on the solution itself at the threshold where from Eqs. (37) and (41) obviously $A\to 0$. In that case we rewrite the solution $X(x)$ of Eq. (33) as

$$X(x) = \frac{a\,\mathrm{dn}(kL,\mu)}{\mathrm{dn}(k(x-L),\mu)}, \tag{44}$$

expand the denominator, take the limit $L\to\infty$ first, and then make $\mu\to 1$. We obtain $X(x)$ of Eq. (33) as

$$X(x) \underset{L\to\infty}{\longrightarrow} a_s\,\mathrm{sech}(kx). \tag{45}$$

The same procedure applied to $T(t)$ in Eq. (32), with $\nu\to 0$, provides

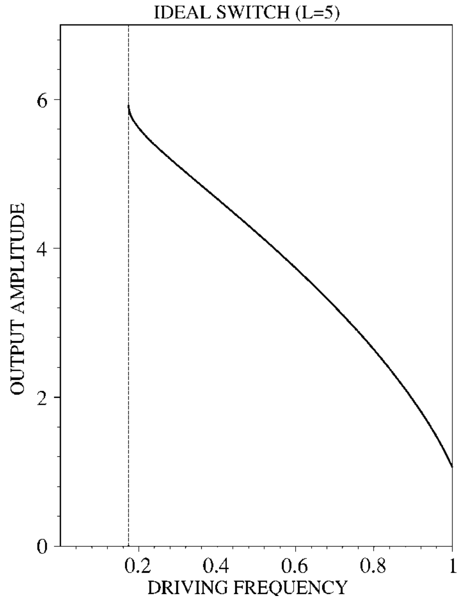

FIG. 3. Output amplitude 4 arctan(A) when $a=0$ as a function of Ω for $L=5$ obtained from Eq. (48) by solving Eq. (47).

$$T(t) \underset{L\to\infty}{\longrightarrow} \cos[\omega(t-t_0)], \tag{46}$$

and the resulting solution $u(x,t)$ of sine-Gordon on the semi-line is the stationnary breather centered in $x=0$ accordingly with Ref. [7].

B. Ideal switch

Considering the type I solution, expression (17) that links the input a to the output A can produce $a=0$ with $A\neq 0$, such as to generate a regime of nonvanishing output value with a vanishing input amplitude, the ideal switching regime. This is the case when

$$kL = \mathbb{K}(\mu), \quad \Omega\mathbb{K}(\nu) = \frac{\pi}{2}\omega, \tag{47}$$

where A, μ, and ν are related to ω and k through Eq. (18). Note the formal analogy with Eq. (40) where the parameters A, μ, and ν are different.

This is a system of equations for $\{\omega,k\}$ whose solution then produces the seeked output amplitude by

$$A^2 = \frac{1-\omega^2+k^2}{1+\omega^2-k^2}, \tag{48}$$

defined by Eq. (47) in terms of the physical entries L and Ω. We have plotted in Fig. 3 the output amplitude 4 arctan A in the ideal switching case ($a=0$) as a function of Ω for length $L=5$.

We observe that, for a given length, there exists a threshold in frequency below which no ideal switching is allowed. This is understood by observing that A^2 diverges when $\omega^2 \to k^2-1$, for which $\mu\to 1$ [a limit threshold that has exactly the same origin as in Eq. (41) when $L\to\infty$]. Conversely, at given driver frequency Ω, there exists a minimum length L of the medium to obtain an ideal switch, it is displayed in

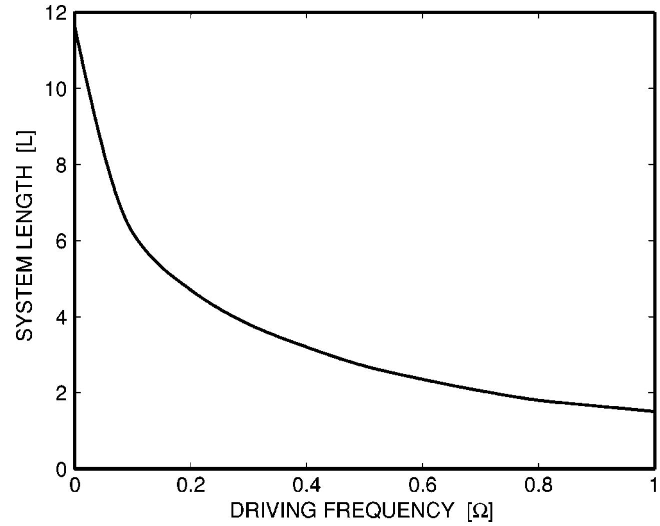

FIG. 4. Minimal length of the system below which one does not have ideal switch [the solution of Eq. (47) ceases to exist].

Fig. 4. Let us remark that the notion of nonlinear dispersion relation is not useful to predict, at given driving frequency Ω, the minimum driver amplitude that generates transmission, as indeed we have here an example where this minimum is simply vanishing.

IV. NUMERICAL SIMULATIONS

A. Damping and boundary driving

Bistable properties, and in particular ideal switching, have been analytically described in the integrable case (1). However, any realistic physical situation must take into account the damping inherent to the medium. The simplest way to include damping is to assume the model

$$u_{tt} + \gamma u_t - u_{xx} + \sin u = 0, \tag{49}$$

associated with the initial-boundary value problem (2) in the particular subclass (3). We study here the bistable properties

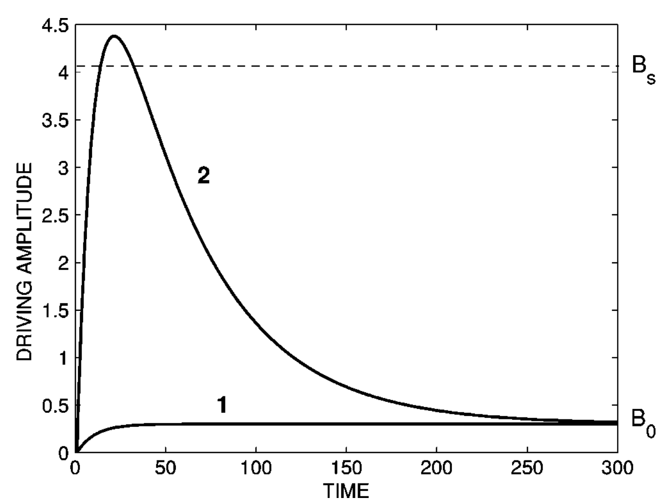

FIG. 5. Two different paths for driving the sine-Gordon system. B_0 is the driving amplitude in the stationary regime and B_s is a supratransmission threshold.

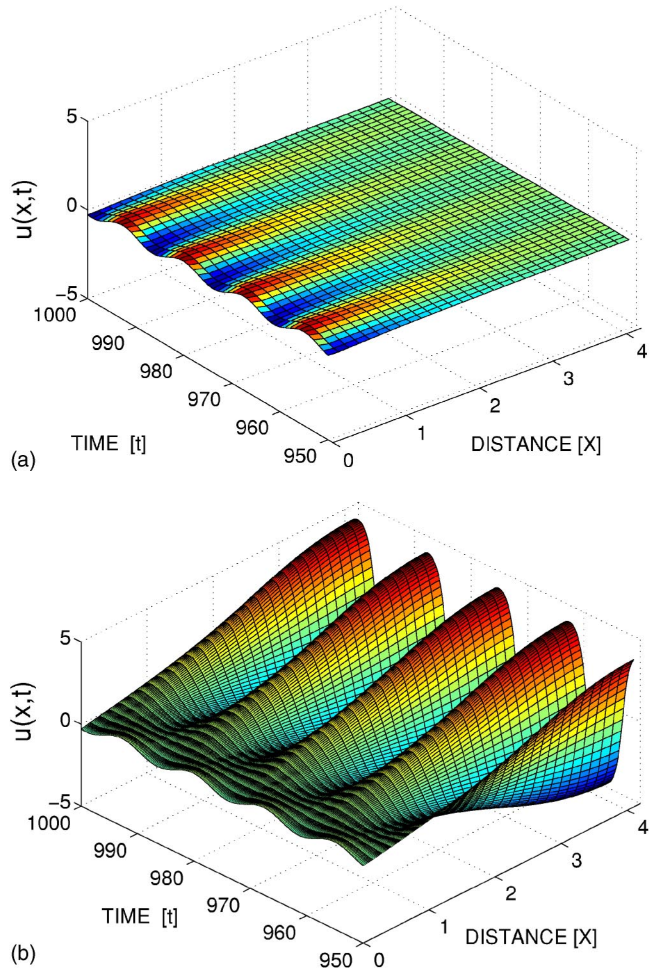

FIG. 6. Three-dimensional plots of the sine-Gordon system dynamics after having reached stationary regime. Upper plot corresponds to the driving path 1 of Fig. 5 and lower plot to path 2. In both cases driving frequency is $\Omega=0.5$, stationary driving amplitude $B_0=0.3$, damping coefficient $\gamma=0.01$, and system length $L=4.1$.

of Eq. (49) by numerical simulations and compare the results to the analytical predictions.

To that end the system is driven at the input boundary $x=0$ with a bandgap frequency and time-dependent amplitude as follows: in a first numerical simulation, the amplitude is smoothly increased up to the value B_0 smaller than the supratransmission threshold B_s. In a second simulation, the amplitude is increased up to a value exceeding the supratransmission threshold and then, after a time sufficient to generate moving breathers, it is decreased to the same value B_0 as in the first case. Figure 5 displays the two time variations of the driving amplitude that we have used in the numerical simulations. After having reached a stationary regime, although the driving amplitudes B_0 are equal in both cases, the dynamics drastically differ in those two cases as it is expected from the analytical consideration presented above and described hereafter.

B. Evidence of bistability

In most of our numerical simulations we choose the driving frequency in the middle of the band gap $\Omega=0.5$, use

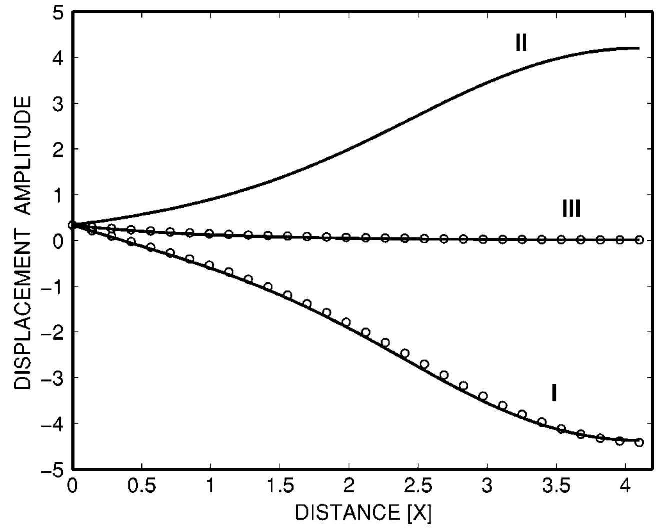

FIG. 7. Comparison of analytical expressions (solid lines) for the profiles of standing waves (14), (26), (33), corresponding to solutions of types III, II, and I, respectively, and numerical simulations (circles). The type III solution is reached along path 1 of Fig. 5 while the type I results from path 2. The type II solution, unstable, is never reproduced by the system.

damping parameter $\gamma=0.01$ and length $L=4.1$. For the driving amplitude along path 1 in Fig. 5, we always observe a stationary regime with decaying profile of the standing wave, very well described by the exact analytical solution of type III (32), (33). Instead, when driving along path 2, we get the picture corresponding to the exact type I solution (13), (14). Those two drastically different behaviors of the system are displayed as three-dimensional plots in Fig. 6.

It is remarkable on the second picture of Fig. 6 that the system has locked to a stationary solution with a small driving amplitude (here $B_0=0.3$) and a large output amplitude (evaluated at $B=4.35$). Let us mention that we can drive the system with amplitudes down to $B_0=0.1$ and still have the type I solution (large output amplitude) despite presence of damping in the system, getting thus a regime of almost ideal switch, or almost perfect detector.

Another remark is that the system never locks to the exact solution of type II (25), (26), simply because this solution is unstable. For instance, if that exact solution is used as an initial condition in the sine-Gordon equation, it eventually breaks down.

To be complete, we compare the analytical expressions of the standing waves profiles of Eqs. (14), (26), and (33) to the results of numerical simulations in the case of the two different driving paths in the context of Fig. 6. The result is displayed in Fig. 7, where the obtained perfect matching shows that indeed the system locks to the analytical solution obtained by assuming frequency synchronization and amplitude matching. This is completed by plotting in Fig. 8 the input-output amplitude dependence obtained from numerical simulations and its comparison with analytical curves derived from formulas (17), (29), and (36).

C. Energetic considerations

The physically useful bistable nature of the system manifests in large difference between the energy dissipation in the

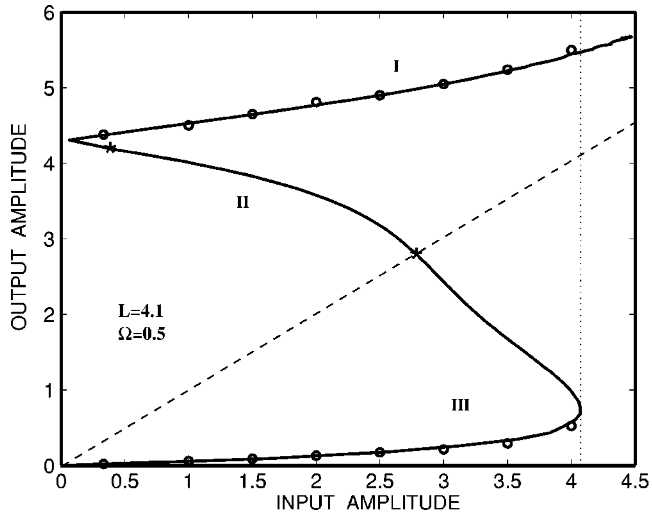

FIG. 8. Comparison of input-output amplitude dependence obtained from numerical simulations (circles) with analytical curves derived from formulas (17), (29), (36).

two stationary regimes. The averaged energy released from the driver in unit time, can be expressed as

$$P = \frac{\Omega}{2\pi}\int_0^{2\pi/\Omega} dt \int_0^L dx\ \gamma u_t^2. \tag{50}$$

Indeed one can easily obtain

$$\frac{\partial}{\partial t}\int_0^L dx\,\mathcal{H} = -\int_0^L dx\ \gamma u_t^2 - (u_x u_t)|_{x=0},$$

$$\mathcal{H} = \frac{1}{2}u_t^2 + \frac{1}{2}u_x^2 + 1 - \cos u, \tag{51}$$

which by averaging on one period furnishes Eq. (50) as the boundary value in $x=0$ is periodic.

Although the analytical solution of the sine-Gordon equation (1) are not solutions of the damped version (49), we may compare the power defined above obtained by numerical simulations of Eq. (49) to the expression (50), where u is simply replaced by the exact solution (type III before the switch, type I after). The result of this comparison is displayed in Fig. 9 where we see that expression (50) with analytical solutions fit strikingly well the numerical simulations, and that the power P after the switch is 2 to 3 orders of magnitude greater than before the switch.

V. COMMENTS AND CONCLUSION

It is worth mentioning that while the analytical solution of type I holds for any length L, in a realistic physical system (nonzero damping), the situation is different. In particular, for large L and low driving amplitudes, when several nodes of the type I standing wave solution are present, the solution cannot survive and decays to a type III solution. This is understood by the following simple argument: all of the exact solutions derived in the previous sections are standing waves, i.e., they do not generate energy flux. Thus, regions of the system far from the boundary cannot gain energy from the driver and the oscillations will eventually fade away.

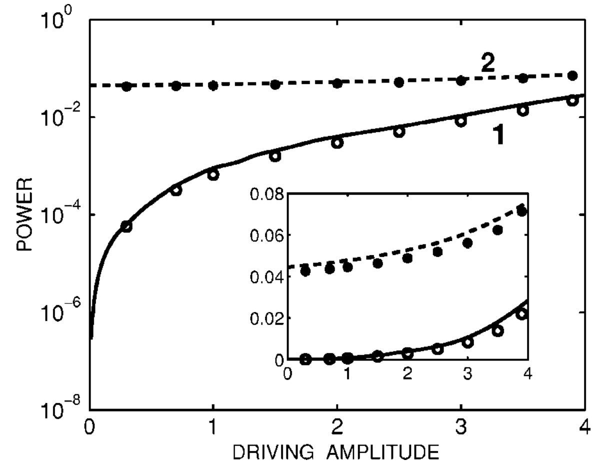

FIG. 9. Power P of Eq. (50) in terms of the driving amplitude in lin-log (main plot) and lin-lin (inset) scales. Solid line [solutions (13) and (14)] and circles (simulations) correspond to driving regime 1 of Fig. 5. Dashed line [solutions (32) and (33)] and asterisks (simulations) result from driving regime 2. Length is $L=4.1$, driving frequency $\Omega=0.5$, and damping coefficient $\gamma=0.01$.

We have essentially demonstrated, both by analytical and numerical treatment, that the bistable property on the sine-Gordon system allows one to generate a particular regime that works as an ideal switch: nonzero output for vanishing input. In a realistic physical system (including damping) the property is conserved but for small (nonvanishing) input. This nonlinear hysteresis has been shown to correspond to quite determinant differences in the power released by the driver to the system.

ACKNOWLEDGMENTS

It is a pleasure to thank Yu. S. Kivshar for the useful information regarding the recent experiments on bifurcations in Josephson junctions. One of us (R.Kh.) aknowledges the support of France-NATO, and thanks the ICTP of Trieste for hospitality.

[1] H. G. Winful, J. H. Marburger, and E. Garmire, Appl. Phys. Lett. **35**, 379 (1979).
[2] I. Siddiqi, R. Vijay, F. Pierre, C. M. Wilson, L. Frunzio, M. Metcalfe, C. Rigette, R. J. Schoelkopf, M. H. Devoret, D. Vion, and D. Esteve, Phys. Rev. Lett. **94**, 027005 (2005).
[3] S. R. Shenoy and G. S. Agarwal, Phys. Rev. Lett. **44**, 1524 (1980).
[4] A. V. Ustinov, Physica D **123**, 315 (1998).
[5] D. Barday and M. Remoissenet, Phys. Rev. B **41**, 10 387 (1990).
[6] Yu. S. Kivshar, O. H. Olsen, and M. R. Samuelsen, Phys. Lett. A **168**, 391 (1992).
[7] F. Geniet and J. Leon, Phys. Rev. Lett. **89**, 134102 (2002).
[8] F. Geniet and J. Leon, J. Phys.: Condens. Matter **15**, 2933 (2003).
[9] R. Khomeriki, Phys. Rev. Lett. **92**, 063905 (2004).
[10] J. Leon and A. Spire, Phys. Lett. A **327**, 474 (2004).
[11] G. Costabile, R. D. Parmentier, B. Savo, D. W. McLaughlin, and A. C. Scott, Appl. Phys. Lett. **32**, 587 (1987).
[12] P. F. Byrd and M. D. Friedman, *Handbook of Elliptic Integrals for Engineers and Physicists* (Springer, Berlin, 1954).